Supplement of Nat. Hazards Earth Syst. Sci., 25, 991–1012, 2025
https://doi.org/10.5194/nhess-25-991-2025-supplement

Natural Hazards and Earth System Sciences
Open Access

Supplement of

Towards a harmonized operational earthquake forecasting model for Europe

Marta Han et al.

Correspondence to: Marta Han (marta.han@sed.ethz.ch)

S1. Data

This section includes two figures referred to in the dataset description. Both are outputs of ESHM20 (Danciu et al., 2021), and only used as input to our proposed models. Figure S1 shows changes in m_c through time for all 47 regions in the catalog, demonstrating the spatial differences present at any given time point. As mentioned in Sect. 2, the reduction in spatial variation in m_c to one order of magnitude in 1980s is the reason for selecting our training catalog to start in 1990, with data between 1980 and 1990 used as auxiliary training set. Further reduction in spatial variation post-2005 also showcases effects of incompleteness in Sect. 4.2.

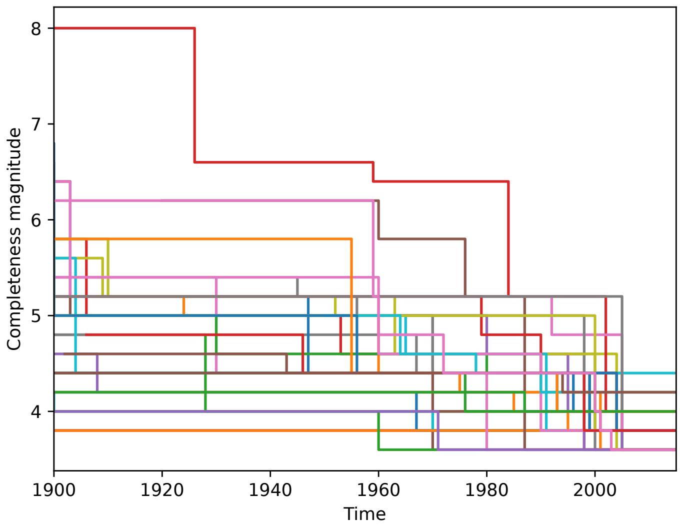

Figure S1. Completeness levels assessed in ESHM20 through time, each colored line represents one of the 47 administrative regions in the catalog.

Figure S2 shows the rate map given as input to ETAS variants trained in our study. The rates are normalized before being used in the parameter inversion as overall background rate multiplying them is also an inverted parameter. Spatial variation is also used to draw locations of simulated background events during the simulation phase.

S2. Results of consistency tests

In Figure 4, we show retrospective cumulative counts of events simulated by ETAS variants fitted on the European dataset. For comparison, we show the same for $\text{ETAS}_{\text{USGS}}$ in Figure S3, but not in the main figure since this model is only there as an additional benchmark with global parameters set, and not fitted to the European dataset.

S3. Results of pseudo-prospective tests

Figure S4 shows the cumulative information gain as displayed in Figure 6(a), only for varying water levels ranging from extremely high to low values, demonstrating its effect on the comparison to the time-independent model. The implications are discussed in Sect. 4.3.

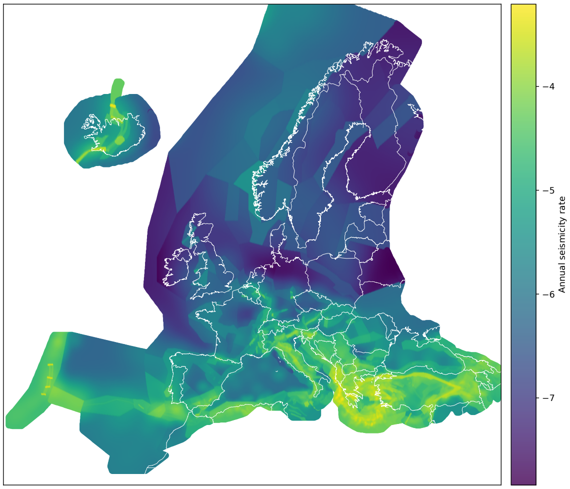

Figure S2. Annual seismicity rates per spatial bin obtained by combining the area sources model and the background seismicity and active faults model with equal weighting (Danciu et al., 2021).

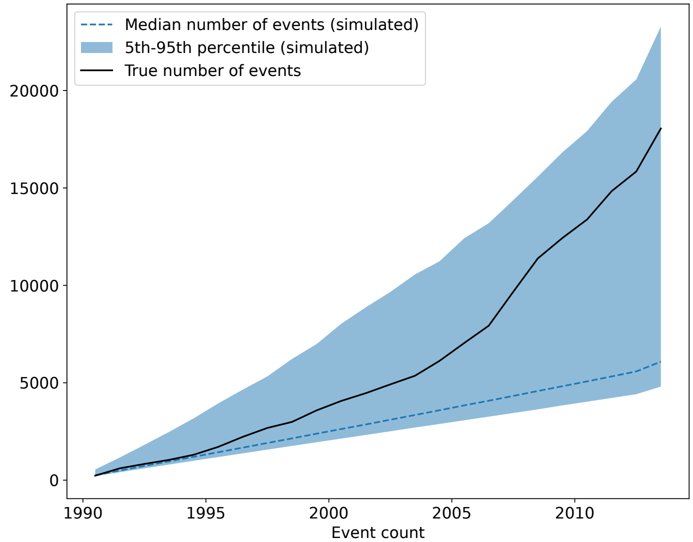

Figure S3. Cumulative count of events simulated for the retrospective forecasts by $ETAS_{USGS}$, continuation of Figure 4.

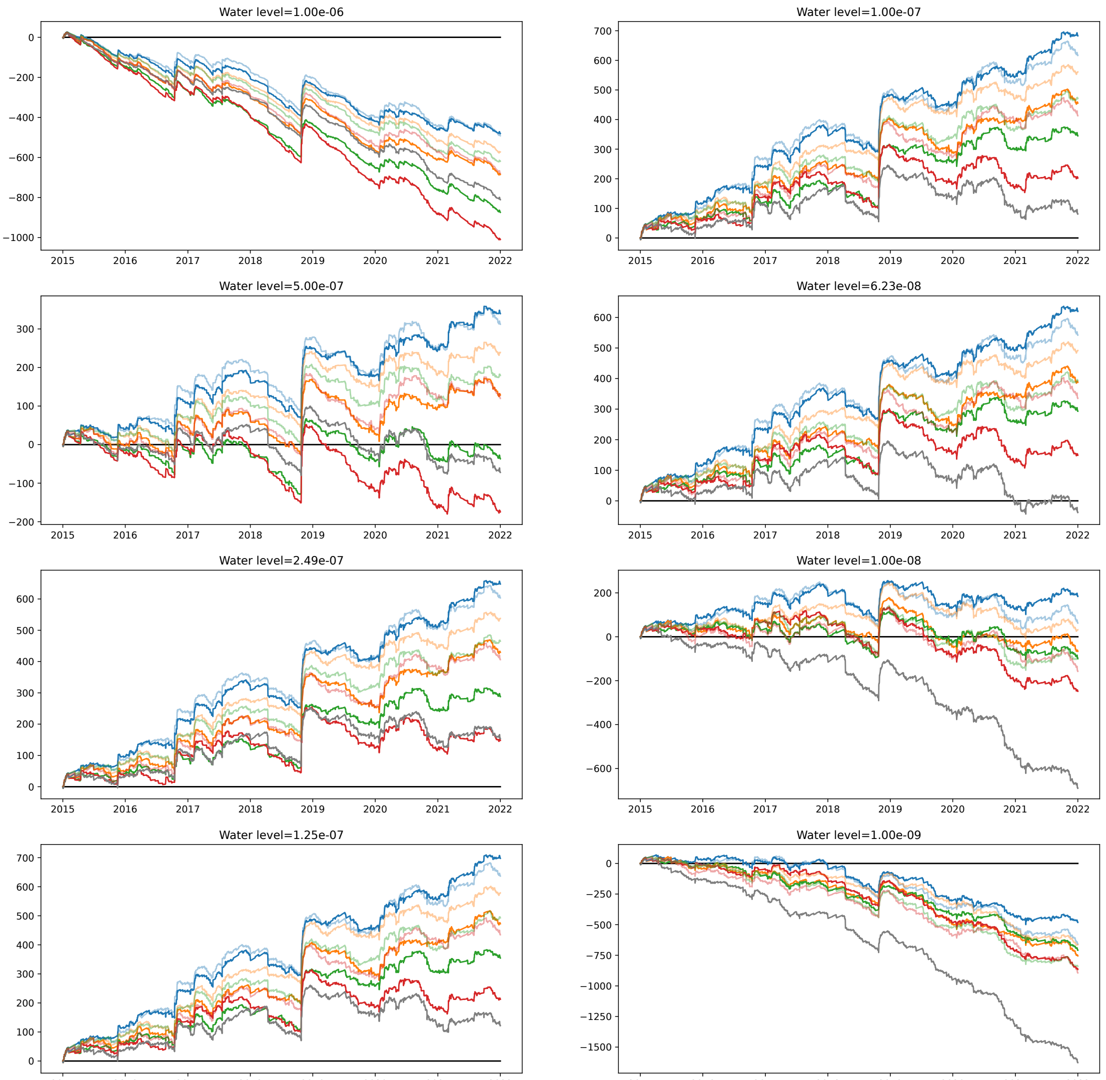

Figure S4. Cumulative information gain through time, for consecutive non-overlapping 1-day windows over 7 years in the validation catalog. All models are compared to the Poissonian time-independent model, which acts as the null model. Spatial binning of 0.1°lat $\times$ 0.1°lon is applied.

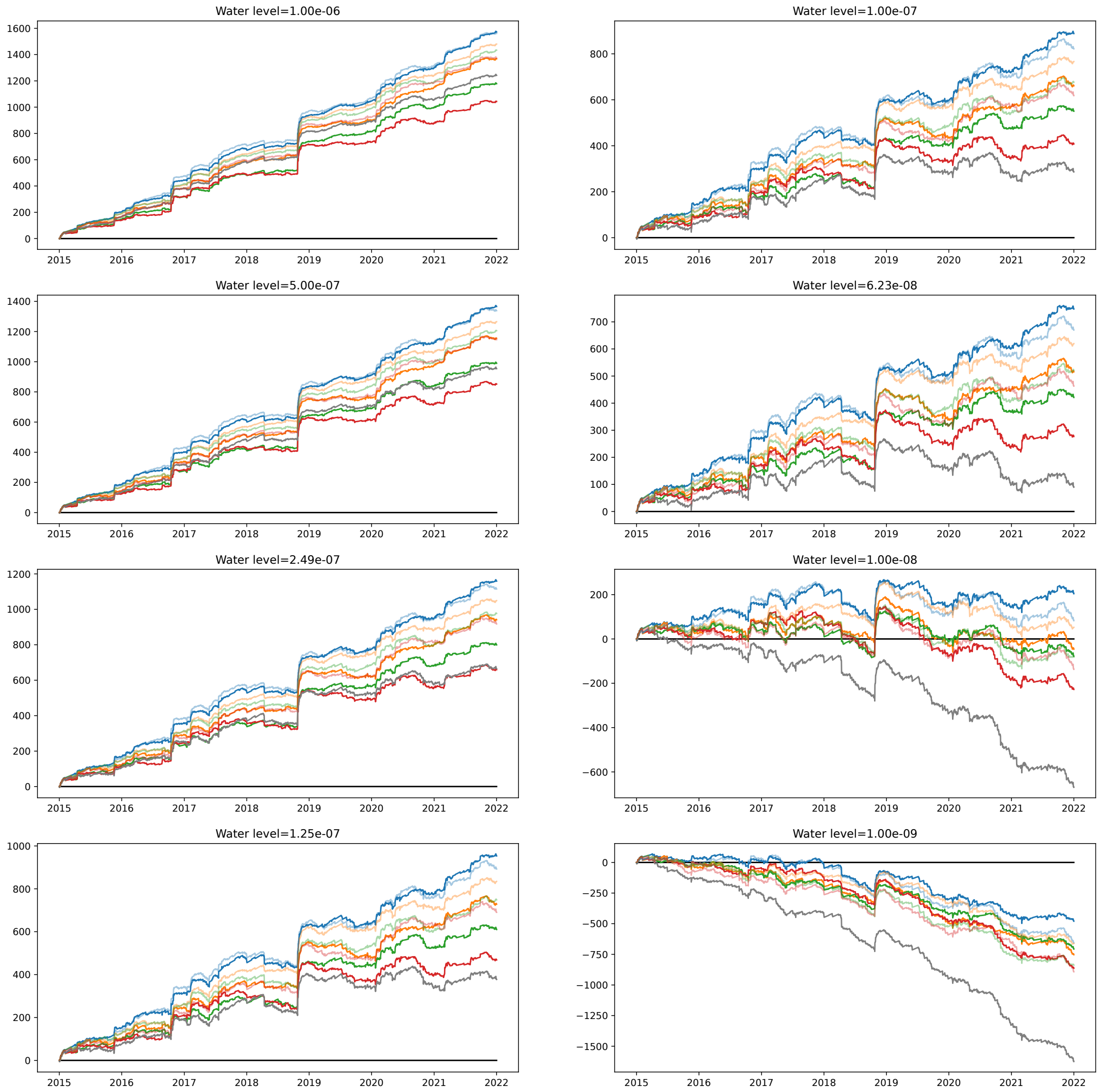

Figure S5. Cumulative information gain through time, for consecutive non-overlapping 1-day windows over 7 years in the validation catalog. All models are compared to the Poissonian time-independent model, which acts as the null model. Spatial binning of 0.1°lat $\times$ 0.1°lon is applied. Unlike in Figure S4, water level is only applied in bins when none of the simulations produce the observed number of events in a spatial bin.

Figure S5 shows the cumulative information gain for varying water levels ranging from extremely high to low values as in Figure S4, only in this case only using the water level when it is necessary, meaning when the bin representing the observed number of events is empty according to simulations. Relevant discussion is again in Sect. 4.3.

References

Danciu, L., Nandan, S., Reyes, C. G., Basili, R., Weatherill, G., Beauval, C., Rovida, A., Vilanova, S., Sesetyan, K., and Bard, P.-Y.: The 2020 update of the European Seismic Hazard Model-ESHM20: Model Overview, EFEHR Technical Report, 1, publisher: ETH Zurich, 2021.